JBAAR

Journal of Bioscience and Applied Research

https://jbaar.journals.ekb.eg

SPBH

# End-to-end test for brain single and fractionated stereotactic radiotherapy using the LUCY 3D phantom

**Adeb A.S.A. Almaamari[1,2], Y. Adib[3], M. A. Youssoufi[1], M. Driouch[4], S. Boutayeb[1], H. Elkacemi[1,2], T. Kebdani[1,2], K. Hassouni[1,2]**

[1]Department of Radiotherapy, National Institute of Oncology, UHC Ibn Sina, Rabat, Morocco.

[2]Faculty of Medicine, Mohammed V University, Rabat, Morocco.

[3]LPHE-MS, Faculty of Science, Mohammed V University, Rabat, Morocco.

[4]LPMS, Faculty of sciences, Ibn tofail University, Kenitra, Morocco.

**Corresponding Author: Adeb A.S.A. Almaamari E-mail:** adeebalmamari66@gmail.com

**ORCID** ID: 0009-0006-8174-2509

**DOI: 10.21608/jbaar.2025.451070**

## Abstract

Stereotactic Radiosurgery is nowadays the main radiotherapy treatment used for small-sized diseases located within the brain. Given the highest complexity related to this technique, periodic tests are mandatory to ensure an efficient workflow is correctly implemented. Our study aims to perform an end-to-end quality assurance test for brain stereotactic radiosurgery using the Lucy 3D QA phantom. CT-images of Lucy phantom were acquired following the same H&N CT-protocol simulating real real-world scenario, with a plugged Pinpoint 3D ionization chamber. A dose distribution was calculated on DICOM images and taken as the gold standard for subsequent comparison with the measured dose under the VersaHD LINAC. 10 patients, noted P1 to P10, were selected and classified as two cohorts based on the prescribed dose (i.e., 5 patients with 20 Gy, and 5 patients with 27 Gy prescribed dose) and one lesion with a maximum diameter less than 5cm. Errors ranged from -5.49% for the P10 to 3.55% for P8, which were both with 27Gy as prescribed dose. Maximum and minimum doses within the ionization chamber's active volume range from 15.249 Gy for P4 and 21.171 Gy for P6 to 23.418 Gy for P3 and 32.282 Gy for P8, for patients with 20 Gy and 27 Gy prescribed dose, respectively. The difference Max-min ranges from 4.3 Gy for P10 to 12.052 Gy for P4. Our findings show that all of the selected plans respect the adopted tolerance, with small errors that could be caused by the user or material performance, which add additional errors to the final analyzed result.

**Keywords:** Stereotactic Radiosurgery, Lucy 3D QA phantom, CT-images, Pinpoint 3D.

---

## 1 Introduction

Modern intensity modulation-based radiotherapy techniques, such as Intensity modulated radiotherapy (IMRT) and Volumetric Modulated Arc Therapy (VMAT), provide high-quality treatment plans in terms of dose distribution conformity to target volume and highly spared organ at risk (OAR) [1, 2]. These techniques are beneficial when treating tumors with moderate and larger volumes, such as prostate, lung, or brain cancers [3, 4]. Stereotactic radiosurgery (SRS) is a highly precise form of radiation therapy used primarily to treat tumors, abnormalities, and other issues within the central nervous system (CNS), such as the brain and spine [5, 6]. Unlike traditional

Received: April 3, 2025. Accepted: July 28, 2025. Published: August 25, 2025

surgery that consists of totally removing the tumor volume, SRS is a non-invasive procedure that uses thin beams of high-dose radiation to target specific areas without damaging as maximum as possible, surrounding healthy tissues, resulting in low toxicity, if not, it remains acceptable, and higher local tumor control [7, 8].

SRS is valued for its precision, accuracy, and effectiveness, often allowing patients to avoid the risks and recovery time associated with conventional surgery [9]. The treatment is typically completed in a single session, though multiple sessions may be necessary for clinical indications, in which case it is called fractionated stereotactic radiotherapy (SRT) [10]. The technique is commonly delivered using advanced systems such as the Gamma Knife, Cyber Knife, and traditional medical linear accelerators (LINAC), equipped with specific devices such as thin multi-leaves collimators [11, 12]. Stereotactic radiosurgery is a precise method in neurosurgery used to target specific brain areas. Despite its benefits, concerns exist about accuracy, potential risks, and long-term outcomes that require efficient quality assurance programs to be clinically implemented [13].

Given the complex treatment process in radiotherapy, in which numerous uncertainties could be raised, which requires a unique quality control test for each treatment step, this is what we call a *component-by-component* test. On the other hand, an *End-to-End* test consists of simulating a real treatment process in terms of patient anatomy using anthropomorphic phantoms during CT imaging, exporting DICOM files to the treatment planning system (TPS) for dose calculation, and phantom irradiation under LINAC simulating a realistic patient treatment process. This is what we call an *end-to-end* test, in which the final uncertainty between the calculated and measured

Data reflects on the entire chain error instead of each step separately [14- 16].

Currently, multiple end-to-end quality assurance programs are implemented using a variety of phantom geometries with multiple detectors, including the use of Gafchromic films for precise dose distribution profiles, thanks to the higher resolution of 2D films [17], Gel dosimeters that provide the measurement of 3D dose distribution [18], in addition to ionization chambers [14]. In our previous work [19], we implemented an end-to-end quality assurance test for Head-and-Neck VMAT treatment plus using an anthropomorphic phantom with optically stimulated luminescence dosimeters (OSLD) in the same institute. The main purpose of our work is to perform an end-to-end test for fractionated stereotactic radiotherapy (SRT) using the Lucy 3D phantom with a pinpoint 3D type ionization chamber, to establish a consensus guideline for institutions and medical physicists when evaluating their own local systems. To the best of our knowledge, no previous work has conducted an end-to-end test by using the Lucy phantom.

## 2 Materials and Methods

### 2.1 Lucy 3D phantom

Lucy$^{TM}$ 3D quality assurance phantom is a broadly used equipment for radiotherapy and imaging, routinely used for different purposes. It consists of a homogeneous PMMA sphere, with 140mm in diameter. Lucy$^{TM}$ phantom contains changeable square inserts with unique usage, and the ensemble is placed on a couch lock platform with a bubble level to precisely align and position the phantom. It may be used for MRI applications with an 85×85×10 mm square insert that contains 3 mineral oil-filled heterogeneous geometries to be viewed by the magnetic field with a known volume and area that will then be fused with the corresponding

CT image for distortion investigation. Electron density-to-Hounsfield Units (ED-to-HU) curve can also be plotted and quickly verified using Lucy$^{TM}$ phantom with 85×85×10 mm square insert that contains 5 different densities to notice Water (the square insert itself), air, trabecular bone, cortical bone, and adipose. The insert used in our study contains a cylindrical hole in which the physicist can plug the ionization chamber in such a way that the active volume is at the exact center of the spherical phantom body.

## 2.2 Patient selection

10 patients underwent brain Stereotactic Radiosurgery (SRS), with one lesion of maximum diameter less than 5 cm, were retrospectively selected for our study. A Clinical Target Volume (CTV) was defined with an expert radio-oncologist, and the corresponding Planning Target Volume (PTV) is defined as an additional margin of 2mm over the CTV (i.e., PTV = CTV + 2mm) for all patients in cooperation with the radiotherapy department medical physicists. Unique doses were prescribed to each patient based on their clinical case indication, such as mono-fractionated treatments. Table 1 below describes the principal treatment planning optimization parameters, including arc number, monitor units per arc, couch and collimator rotation angles, PTV volume, and the maximum diameter for each patient named P1 to P10, which refer to Patient1 to Patient10. The 10 selected patients were split into two categories: the first are those who received a mono-fractionated treatment with a 20 Gy prescribed dose in a unique treatment fraction, the second are those with a total of 27 Gy prescribed to the PTV to be cumulatively received in 3 fractions.

## 2.3 Measurement process

Phantom CT images were first acquired using a Siemens SOMATOM Sensation open scanner (Siemens Medical Solutions, Erlangen, Germany) following the same *Stereo Brain CT* protocol in the department of radiotherapy in the hospital (120 Kvp, tube rotation time of 0.5 seconds, slice thickness of 1.5 mm, tube current modulation set to ”ON”, head-first supine position). External lead markers were put and aligned with CT lasers to precisely localize the treatment isocenter during dose calculations and accurately reposition the phantom on the treatment couch according to the predefined displacements. A Pinpoint type ionization chamber with 0.015 $cm^3$ active volume and a calibration factor of $N_{D,w}$ = 2.392 Gy/C, was plugged into the phantom during CT-imaging.

Phantom CT images in DICOM (Digital Imaging and Communication in Medicine) format were exported to MONACO® Treatment Planning System (TPS) (Elekta, Stockholm, Sweden) v6.11.4 to delineate external *body outline* as patient and ionization chamber active volume, and also to calculate dose distributions using Monte-Carlo algorithm with calculation grid of 2mm considering the treatment couch for posterior beam attenuation and scattered radiation to be included in the final dose distribution. The mean absorbed dose within the contoured ionization chamber volume was compared to measurements based on AAPM Task Group-119 formalism, as shown in Equation 1. Treatment plans were delivered from VersaHD® linear accelerator (Elekta, Stockholm, Sweden), equipped with Agility multi-leaf collimator, which consists of 160 thin leaf and 6D HexaPOD robotic couch, with 6 FFF photon beams and 1200 MU/min maximum dose rate.

$$\Delta_{TPS\text{-}IC}(\%) = \frac{Measurement - Calculation}{Calculation} \times 100 = \frac{D_{IC} - D_{TPS}}{D_{TPS}} \times 100 \quad (1)$$

where $D_{IC}$ and $D_{TPS}$ are the measured and the calculated absorbed dose, respectively. Positive value of $\Delta_{TPS-IC}(\%)$ when $D_{IC} > D_{TPS}$ indicates that IC overestimates the calculated dose, and vice versa.

The 10 selected plans were applied to the phantom as *QA-Plan* in order to maintain the same plan properties in terms of number of control points (CP), MLC segments, and apertures at each CP, and dose rate. All plans were approved and transferred to the LINAC using the MOSAIQ® record-and-verify system (Elekta, Stockholm, Sweden). At the irradiation stage,

The phantom was positioned under the LINAC according to the predefined displacements. Measurements were performed with the same couch and collimator rotations to simulate a real-world scenario. Figure 1 shows the principal steps in the measurement process, including CT-imaging acquisition, dose distribution calculation, irradiation of the phantom under the linear accelerator, and dose measurement for subsequent comparison with the calculated dose using Equation 1.

Table 1: Description of the main parameters included in the 10 treatment plans optimization. This includes the number of arcs, collimator and treatment couch rotation angles, and monitor units for each arc. In addition to the PTV volume in cc and the prescribed dose to each patient

| Patients | Arcs | Collimator ° | Couch ° | MU/Arc | PTV volume (cc) | Prescription (Gy) |
|---|---|---|---|---|---|---|
| P1 | 1 | 0 | 0 | 520 | 29.733 | 20 |
| | 2 | 0 | 345 | 602 | | |
| | 3 | 0 | 330 | 1534 | | |
| | 4 | 0 | 0 | 881 | | |
| | 5 | 0 | 10 | 719 | | |
| P2 | 1 | 20 | 0 | 1034 | 4.693 | 20 |
| | 2 | 30 | 7 | 1135 | | |
| | 3 | 330 | 350 | 955 | | |
| P3 | 1 | 0 | 0 | 2270 | 16.955 | 20 |
| | 2 | 0 | 15 | 575 | | |
| | 3 | 0 | 30 | 1089 | | |
| P4 | 1 | 0 | 0 | 1652 | 2.84 | 20 |
| | 2 | 0 | 350 | 618 | | |
| | 3 | 0 | 340 | 1015 | | |
| P5 | 1 | 20 | 0 | 1755 | 1.512 | 20 |
| | 2 | 110 | 20 | 1373 | | |
| | 3 | 340 | 350 | 1116 | | |
| P6 | 1 | 90 | 0 | 186 | 3.842 | 27 |
| | 2 | 20 | 4 | 950 | | |
| | 3 | 340 | 8 | 1258 | | |
| | 4 | 20 | 356 | 687 | | |
| | 5 | 340 | 352 | 939 | | |
| P7 | 1 | 0 | 10 | 215 | 5.375 | 27 |
| | 2 | 90 | 45 | 263 | | |
| | 3 | 90 | 90 | 324 | | |
| | 4 | 90 | 315 | 271 | | |
| | 5 | 0 | 350 | 209 | | |
| P8 | 1 | 0 | 10 | 279 | 38.31 | 27 |
| | 2 | 90 | 30 | 189 | | |
| | 3 | 90 | 60 | 903 | | |
| | 4 | 0 | 0 | 725 | | |
| P9 | 1 | 0 | 350 | 381 | 38.628 | 27 |
| | 2 | 0 | 10 | 355 | | |
| | 3 | 0 | 0 | 407 | | |
| P10 | 1 | 20 | 50 | 261 | 3.199 | 27 |
| | 2 | 20 | 10 | 223 | | |
| | 3 | 20 | 310 | 295 | | |
| | 4 | 20 | 0 | 236 | | |

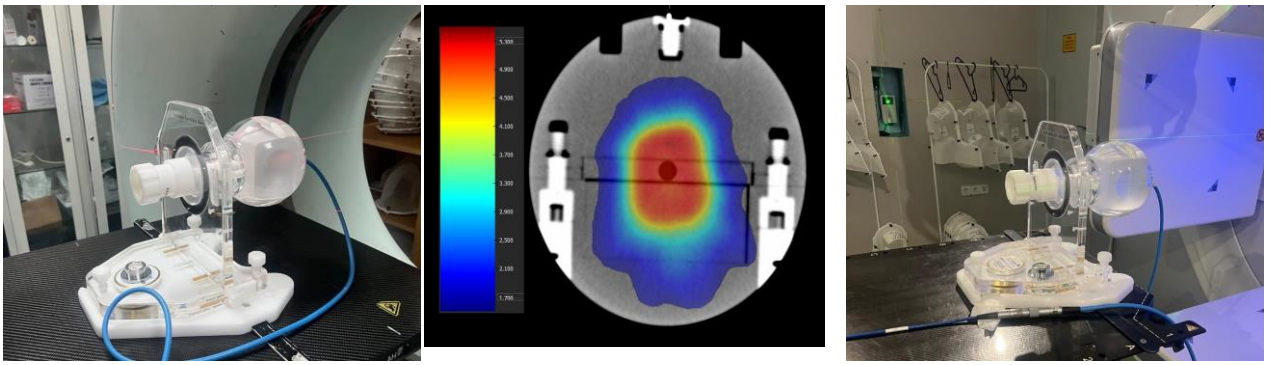

Figure 1: Realistic photos showing the main process steps, including Lucy phantom during CT imaging and DICOM extraction (left), dose distribution calculation on phantom DICOM images showing the used insert and ionization chamber placement (middle), plans administration for dose distribution measurement, with plugged Pinpoint type ionization chamber (right)

## 3 Results

Table 2 below lists calculated dose distribution statistics in terms of min, Max, difference min-max, in addition to the mean dose calculated by the treatment planning system for each treatment plan within the ionization chamber's active volume in *Gray* (Gy). Also, the mean measured dose at the irradiation stage under the linear accelerator is denoted $D_{IC,}$ meaning dose with ionization chamber in Gy. In addition, the percentage difference $\Delta_{TPS-IC}(\%)$ was calculated by using equation 1, mentioned above, between the measured and calculated dose, in order to investigate if the delivered plan meets or exceeds recommended tolerances. In our study, we adopt 5% acceptance criteria given the harder and numerous included uncertainties.

The main adopted analysis in our study is the percentage difference, which ranges from -5.49% for patient P10 to 3.55% for patient P8. As a function of the prescribed dose to the target volume, we notice that $\Delta_{TPS-IC}(\%)$ of patients with 20 Gy ranged from -3.77% for P3 to 2.81% for P4. On the other hand, the maximum variation ranges are observed for those patients with a 27 Gy prescribed dose. Which leads to the fact that the harder the delivered dose, the higher the percentage difference $\Delta_{TPS-IC}(\%)$. Over the 10 plans, 6 plans were measured with an under-estimated dose due to the minus sign in the $\Delta_{TPS-IC}(\%)$.

Table 2: Measured mean point dose compared to TPS calculations for brain Stereotactic radio-surgery (SRS) with one lesion performed in Lucy 3D phantom with pinpoint type 3D ionization chamber

| Patient | $D_{TPS}$ (Gy) | | | | $D_{IC}$ (Gy) | $\Delta_{TPS-IC}$ (%) |
|---|---|---|---|---|---|---|
| | Min | Max | Max-Min | Mean | | |
| P1 | 18.837 | 25.747 | 6.91 | 20.02 | 19.54 | -2.39 |
| P2 | 17.799 | 26.199 | 8.4 | 19.9 | 20.3 | 2.01 |
| P3 | 17.056 | 23.418 | 6.362 | 21.2 | 20.4 | -3.77 |
| P4 | 15.249 | 27.301 | 12.052 | 20.23 | 20.8 | 2.81 |
| P5 | 17.113 | 24.181 | 7.068 | 19.95 | 20.5 | 2.75 |
| P6 | 21.171 | 30.961 | 9.79 | 27.8 | 26.7 | -3.95 |
| P7 | 25.826 | 32.194 | 6.368 | 26.98 | 26.14 | -3.11 |
| P8 | 23.588 | 32.282 | 8.694 | 25.3 | 26.2 | 3.55 |
| P9 | 23.374 | 29.707 | 6.333 | 27.21 | 26.74 | -1.72 |
| P10 | 25.818 | 30.118 | 4.3 | 27.84 | 26.31 | -5.49 |

The maximum and minimum dose within the ionization chamber's active volume ranges from 15.249 Gy for P4 and 21.171 Gy for P6, to 23.418 Gy for P3 and 32.282 Gy for P8, for patients with 20 Gy and 27 Gy prescribed dose, respectively. On the other hand, the difference between the maximum and minimum dose (i.e., Max-Min) that describes the dose range, or otherwise dose heterogeneity, within the ionization chamber ranges from 4.3 Gy for P10 to 12.052 Gy for P4. These patients are those with dose differences -5.59% which is the lowest difference over all measurements, and P4 is the patient's minimum calculated dose with the highest $\Delta_{TPS-IC}$(%) over all patients with a 20 Gy prescribed dose.

## 4 Discussion

The current study aims to perform and implement a consensus program for end-to-end tests using the Lucy 3D phantom with a pinpoint ionization chamber for mono-brain disease stereotactic radiosurgery. 10 patients were selected and split into 2 cohorts as a function of the prescribed dose (i.e., 20 and 27 Gy) with a maximum diameter less than 5cm.

Percentage differences ranged from -5.49% for the P10 to 3.55% for P8, which had both with 27Gy as prescribed dose. Maximum and minimum dose within the ionization chamber's active volume ranges from 15.249 Gy for P4 and 21.171 Gy for P6, to 23.418 Gy for P3 and 32.282 Gy for P8, for patients with 20 Gy and 27 Gy prescribed dose, respectively. The difference Max-min ranges from 4.3 Gy for P10 to 12.052 Gy for P4.

KM. Alexander et al. [20] have developed a 3D printed head phantom for brain stereotactic end-to-end tests purposes with multiple detector type inserts, including the reference ionization chamber, Gel dosimeter, and Gafchromic EBT3 film. Their findings show good agreement between calculated and measured dose distributions, which were all within 2% when using an ionization chamber. This dose difference (%) begins to increase as a function of PTV diameter, passing from 1cm to 2cm. They also highlighted the effect of choosing an optimal dose calculation grid, knowing that when 1mm×1mm, the dose error increases compared to 2mm×2mm, which highlights the numerous sources of errors included in the final analyzed results. S. Maya et al. [21], on the other hand, used a RUBY head phantom for an SRS end-to-end test for mono and multi-metastases treatment using a Pinpoint 3D type 31022 ionization chamber. Their finding pointed out a maximum percentage deviation of less than 3% when verifying mono brain lesions. However, for multi-brain metastases, the percentage deviation of the calculated dose compared to measurements exceeded 10%, because the measurement detector was placed at the metastasis's barycenter (i.e., treatment isocenter and not each lesion separately). B. Ivan and co-authors [22] performed an end-to-end test for SRS using an in-house built block phantom having approximate dimensions of a human head, to compare dose calculation against measurements. They found an average error ranging from 0.5 ± 1.6% to 4.8 ± 2.6 %, and a maximum error ranging from 2.8% to 9.0% as a function of field size and total Monitor Units (MU) for 10 singles 360°arcs SRS treatment plans. However, the average error significantly decreased to 0.3 ± 2.0% and a maximum dose error of 3.1% when using 9 singles 160°arcs instead of one single arc, highlighting the fact that numerous sources of errors could impact the delivered dose compared to the TPS calculation.

## 5 Conclusion

End-to-end test is a powerful approach that should be clinically implemented for a more efficient treatment workflow and performance required for real-world scenarios. End-to-end test allows the analysis of the entire treatment chain by simulating a real-world process (CT-imaging, dose calculation, setup, and irradiation under a linear accelerator). Our findings note that no plan exceeded the adopted acceptance tolerance of 5%, except for the last plan, P10, with an error of -5.49%, showing an under-estimation or under-dose of the target, or error caused by phantom positioning and analysis.

**Conflict of interest:** NIL

**Funding:** NIL

## References


[1] Maria Jose Perez-Calatayud, Antonio Vicente Menendez Lopez, Francisco Javier Celada- Alvarez, Antonio Jose Conde-Moreno, Mariola Bernisz, Françoise Lliso, Vicente Carmona, Jose Gimeno-Olmos, Carlos Botella-Asuncion, and Jose Perez-Calatayud. Feasibility and potential advantages using VMAT in SRS metastasis treatments. *Reports of Practical Oncology and Radiotherapy*, 26(1):119–127, 2021.

[2] Xia Deng, Ce Han, Shan Chen, Congying Xie, Jinling Yi, Yongqiang Zhou, Xiaomin Zheng, Zhenxiang Deng, and Xiance Jin. Dosimetric benefits of intensity-modulated radiotherapy and volumetric-modulated arc therapy in the treatment of postoperative cervical cancer patients. *Journal of Applied Clinical Medical Physics*, 18(1):25–31, 2017.

[3] Sherisse Ornella Hunte, Catharine H Clark, Nikolay Zyuzikov, and Andrew Nisbet. Volumetric modulated arc therapy (VMAT): a review of clinical outcomes—what is the clinical evidence for the most effective implementation? *British Journal of Radiology*, 95(1136):20201289, 2022.

[4] Mohamed M. Fathy, Belal Z. Hassan, Reem H. El-Gebaly, and Maha H. Mokhtar. Dosimetric evaluation study of IMRT and VMAT techniques for prostate cancer based on different multileaf collimator designs. *Radiat Environ Biophys*, 62(1):97–106, 2023.

[5] Isabela Peña-Pino and Clark C. Chen. Stereotactic Radiosurgery as Treatment for Brain Metastases: An Update. *Asian Journal of Neurosurgery*, 18:246–257, 2023.

[6] Philip Gilbo, Isabella Zhang, and Jonathan Knisely. Stereotactic radiosurgery of the brain: a review of common indications. *Chinese Clinical Oncology*, 6(2):S14–S14, 2017.

[7] Elodie Guillaume, Ronan Tanguy, Myriam Ayadi, Line Claude, Sandrine Sotton, Coralie Moncharmont, Nicolas Magné, and Isabelle Martel-Lafay. Toxicity and efficacy of stereotactic body radiotherapy for ultra-central lung tumours: a single institution real life experience. *British Journal of Radiology*, 95(1129):20210533, 2022.

[8] Banu Atalar, Teuta Zoto Mustafayev, Terence T. Sio, Bilgehan Sahin, Gorkem Gungor, Gokhan Aydın, Bulent Yapici, and Enis Ozyar. Long-term toxicity and survival outcomes after stereotactic ablative radiotherapy for patients with centrally located thoracic tumors. *Radiology and Oncology*, 54(4):480–487, 2020.

[9] Timothy Lin, Abhinav Reddy, Colin Hill, Shuchi Sehgal, Jin He, Lei Zheng, Joseph Herman, Jeffrey Meyer, and Amol Narang. The Timing of Surgery Following Stereotactic Body Radiation Therapy Impacts Local Control for Borderline Resectable or Locally Advanced Pancreatic Cancer. *Cancers*, 15(4):1252, 2023.

[10] Samuel R. Marcrom, Andrew M. McDonald, Jonathan W. Thompson, Richard A. Popple, Kristen O. Riley, James M. Markert, Christopher D. Willey, Markus Bredel, and John B. Fiveash. Fractionated stereotactic radiation therapy for intact brain metastases. *Advances in Radiation Oncology*, 2(4):564–571, 2017.

[11] Michael Yan, Lori Holden, Michael Wang, Hany Soliman, Sten Myrehaug, Chia-Lin Tseng, Jay Detsky, Mark Ruschin, Michael Tjong, Eshetu G. Atenafu, Sunit Das, Nir Lipsman, Chinthaka Heyn, Arjun Sahgal, and Zain Husain. Gamma knife icon based hypofractionated stereotactic radiosurgery (GKI-HSRS) for brain metastases: impact of dose and volume. *J Neurooncol*, 159(3):705–712, 2022.

[12] Zyad A. Tawfik, Mohamed El-Azab Farid, Khaled M. El Shahat, Ahmed A. Hussein, Ahmed A. Eldib, and Mostafa Al Etreby. A dosimetric study comparing Cyberknife and LINAC-based stereotactic radiotherapy or radiosurgery treatments. *Journal of Radiation Research and Applied Sciences*, 17(1):100781, 2024.

[13] Jun Li, Xile Zhang, Yuxi Pan, Hongqing Zhuang, Junjie Wang, and Ruijie Yang. Assessment of Delivery Quality Assurance for Stereotactic Radiosurgery With Cyberknife. *Front. Oncol.*, 11, 2021.

[14] Pavel Kazantsev, Wolfgang Lechner, Eduard Gershkevitsh, Catharine H. Clark, Daniel Venencia, Jacob Van Dyk, Paulina Wesolowska, Victor Hernandez, Nuria Jornet, Milan Tomsej, Tomislav Bokulic, and Joanna Izewska. IAEA methodology for on-site end-to-end IMRT/VMAT audits: an international pilot study. *Acta Oncologica*, 59(2):141–148, 2020.

[15] Jennifer O'Daniel, Shiva Das, Q. Jackie Wu, and Fang-Fang Yin. Volumetric-Modulated Arc Therapy: Effective and Efficient End-to-End Patient-Specific Quality Assurance. *International Journal of Radiation Oncology, Biology, Physics*, 82(5):1567–1574, 2012.

[16] Viatcheslav V. Zakjevskii, Cory S. Knill, Joseph. T. Rakowski, and Michael G. Sny- der. Development and evaluation of an end-to-end test for head and neck IMRT with a novel multiple-dosimetric modality phantom. *Journal of Applied Clinical Medical Physics*, 17(2):497–510.

[17] S. Pallotta, S. Calusi, L. Marrazzo, C. Talamonti, S. Russo, M Esposito, C Fiandra, F. R. Giglioli, M. Pimpinella, V. De Coste, A. Bruschi, S. Barbiero, P. Mancosu, M. Stasi, and
R. Lisci. End-to-end test for lung SBRT: An Italian multicentric pilot experience. *Physica Medica*, 104:129–135, 2022.

[18] Libing Zhu, Yi Du, Yahui Peng, Xincheng Xiang, and Xiangang Wang. End-to-End QA with Polymer Gel Dosimeter for Photon Beam Radiation Therapy. *Gels*, 9(3):212, 2023.

[19] Youssef Adib, Abdelhak Bouyhamarane, Moulay Ali Youssoufi, Lalla Btissam Drissi, Mohammed Reda Mesradi, Salwa Boutayeb, Mustapha Driouch, Adeb A. S. A. Almaamari, Hanan El Kacemi, Tayeb Kebdani, and Khalid Hassouni. End-to-End patient-specific VMAT quality assurance for common Head-and-Neck cancers using RANDO anthropo- morphic phantom with OSLD. *Radiation Physics and Chemistry*, 230:112543, 2025.

[20] KM Alexander, KH Dekker, T Olding, and LJ Schreiner. End-to-End Quality Assurance of Stereotactic Radiation Therapy Using an Anthropomorphic Head Phantom. *J. Phys.: Conf. Ser.*, 2167(1):012022, 2022.

[21] Maya Shariff, Johanna Grigo, Siti Masitho, Tobias Brandt, Alexander Weiss, Ulrike Lambricht, Willi Stillkrieg, Michael Lotter, Florian Putz, Rainer Fietkau, and Christoph Bert. End-to-end testing for stereotactic radiotherapy, including the development of a multi-modality phantom. *Zeitschrift für Medizinische Physik*, 34(3):477–484, 2024.

[22] Ivan A. Brezovich, Xingen Wu, Richard A. Popple, Elizabeth Covington, Rex Cardan, Sui Shen, John Fiveash, Markus Bredel, and Barton Guthrie. Stereotactic radiosurgery with MLC-defined arcs: Verification of dosimetry, spatial accuracy, and end-to-end tests. *Journal of Applied Clinical Medical Physics*, 20(5):84–98, 2019.